ChemComm

COMMUNICATION

View Article Online
View Journal | View Issue

Cite this: *Chem. Commun.*, 2014, **50**, 1912

Received 17th November 2013,
Accepted 12th December 2013

DOI: 10.1039/c3cc48764d

www.rsc.org/chemcomm

A new type of double-chain based 3D lanthanide(III) metal–organic framework demonstrating proton conduction and tunable emission†

Min Zhu,[ab] Zhao-Min Hao,[ab] Xue-Zhi Song,[ab] Xing Meng,[ab] Shu-Na Zhao,[ab] Shu-Yan Song[a] and Hong-Jie Zhang*[a]

A new type of 3D lanthanide(III) metal–organic framework directly constructed by double-chain motifs was synthesized. It shows a proton conductivity of 1.6 × 10^{-5} S cm^{-1} at 75 °C at 97% RH, and tunable emission including white light.

Metal–organic frameworks (MOFs) have been rapidly developed from the standpoints of both fundamental and applied chemistry, such as gas storage/separation, ion exchange, magnetism, catalysis, and nonlinear optics.[1] Recently, the exciting new opportunities for MOFs as proton-conducting materials have been opened up.[2] These materials require proton carriers, such as H_3O^+, NH_4^+ or H^+ belonging to acid groups or to hydrogen-bond networks. The main advantage of MOFs as proton-conducting materials is their defined structure, providing a useful insight into the proton-conduction pathway and mechanism.[3] In addition, their highly designable nature enables the tunability of MOF structures, further providing an opportunity to control proton conduction. However, application of MOFs in proton-conduction has not been explored as broadly as gas storage and separation. Limited work on the proton conductivity on MOFs has been reported until now.[4]

Another particularly targeted functionality for MOFs is the fine-tuning of the luminescence properties.[5] The lanthanide metal–organic frameworks (LnMOFs) display interesting optical properties such as sharp and intense luminescence, long lifetime, and emission in the primary color range (red, blue and green).[6] A fine-tuning of the color emission of LnMOFs was easily achieved by the simple doping method in the previous reports.[7] Thus, LnMOFs could be excellent tunable and emitting materials upon doping the framework with other elements.

It is worth noting that, combing the two properties in one MOF system would offer a multi-functional material. Although LnMOFs behave as excellent emitting materials, it is also a challenge to obtain proton-conducting LnMOFs. In fact, the proton conduction in LnMOFs is scarce to date. Only two reports could be documented, a 3D PCMOF-5 framework with highly acidic pores for proton-conducting applications[8a] and a lanthanide carboxyphosphonate open-framework exhibiting multifunctional luminescent and proton-conducting properties.[8b] Still, LnMOFs with proton conduction and tunable emission, including white-light emission, have not been reported.

Herein, a tetracarboxylate ligand, *N*-phenyl-*N*′-phenyl bicyclo[2,2,2]-oct-7-ene-2,3,5,6-tetracarboxdiimide tetracarboxylic acid (**L**) (Scheme S1, ESI†), was selected to construct LnMOFs, **[LnL(H$_2$O)$_3$]·2H$_2$O** (abbreviated as **LnL**, Ln = Y, Pr–Yb). All of them are isostructural, verified by the powder XRD patterns (Fig. S1, ESI†). To the best of our knowledge, this is the first LnMOF showing proton conductivity and tunable emission color.

Single-crystal X-ray diffraction analysis reveals that **EuL** consists of a tetracarboxylate ligand, a lanthanide atom, three coordination water molecules and two free water molecules. The Eu^{3+} ion is nine coordinated by six oxygen atoms of the carboxyl groups, and three oxygen atoms from the terminal water molecules, forming a distorted tricapped trigonal prism geometry (Fig. S4, ESI†). Two kinds of coordination exist for the four carboxyl groups: two of them with a chelate type, and one with a bidentate type, leaving a free carboxyl group (Fig. S6b, ESI†). Interestingly, a pair of ligands with the spacers arrange to the opposite sites, forming a "circle"-like unit (Fig. S5 left, ESI†). The shortest O···O distance between them is about 3.969 Å. Besides, adjacent Eu centers are linked by the carboxyl of the bidentate type, showing a binuclear Eu unit (Fig. S5 right, ESI†). The Eu···Eu distance in the binuclear Eu unit is about 5.090 Å. Then the binuclear Eu unit connects a pair of "circle"-like ligands to an infinite double-chain structure (Fig. 1a and b). It should be noted that the double-chains, as functional motifs, arrange along two different directions, and then are cross-linked through Eu–O covalent bonds to a 3D impact structure (Fig. 1c). Each binuclear Eu unit as a six-connection

[a] *State Key Laboratory of Rare Earth Resource Utilization, Changchun Institute of Applied Chemistry, Chinese Academy of Sciences, 5625 Renmin Street, Changchun 130022, China. E-mail: hongjie@ciac.ac.cn; Fax: +86-431-85698041; Tel: +86-431-85262127*

[b] *University of Chinese Academy of Sciences, Beijing, 100049, China*

† Electronic supplementary information (ESI) available. CCDC 971185. For ESI and crystallographic data in CIF or other electronic format see DOI: 10.1039/c3cc48764d

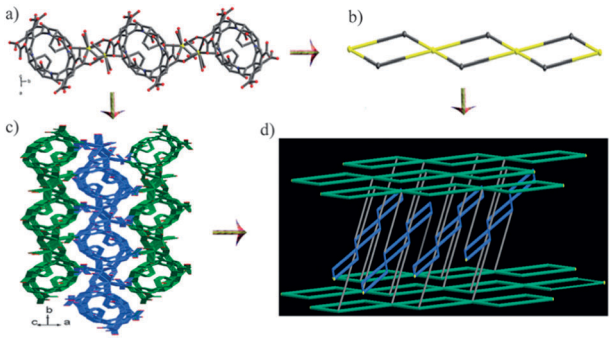

Fig. 1 (a) View of the double-chain structure; (b) the schematic view of the double chain (yellow balls, binuclear Eu units; gray balls, ligands); (c) the three-dimensional (3D) metal–organic framework; (d) the schematic view of the 3D structure.

node and each ligand could be considered as a three-connecting node, bridging three binuclear Eu units. The topological analysis was performed using the TOPOS program,[9] which reveals a (3, 6)-connected alb-3-type topology (Fig. 1d). The vertex symbol is $\{4\cdot8^2\}_2\{4^2\cdot8^{11}\cdot10^2\}$.

The proton conductivities of **EuL** and **DyL** were measured from 25 to 75 °C at approximately 97% RH. They show a similar conduction behaviour. Nyquist plots of **EuL** and **DyL** from 25 to 75 °C are shown in Fig. 2a and Fig. S9a (ESI†). In the temperature range, although the complex impedance plot shows a single semicircle in the high-frequency region, it has two relaxation processes. At 25 °C, the complex modulus plot makes this clear, giving two depressed semicircles (Fig. S7, ESI†). The data were fit by two series of parallel RC circuit $(R_bCPE_b)(R_{gb}CPE_{gb})$[10] (where R_b is the resistance of proton transfer in the bulk phase and CPE is contributions to account for the depressed, *versus* perfect, semicircle due to non-ideal capacitance). Because the sample was a powder crystal, one is attributed to the bulk phase and the other to the grain boundary (g.b.).[11] The unobvious tail at low frequencies may be due to mobile ions being blocked by the electrode–electrolyte interfaces and/or electrode polarization.[2b] R_b is estimated by fitting experimental profiles, and the bulk proton conductivities at room temperature for **EuL** and **DyL** are 1.0×10^{-7} and 1.52×10^{-7} S cm^{-1}, respectively. As the temperature increases, the conductivities for the bulk phase and grain boundary gradually increase (Fig. S8 and S9b, ESI†). At 75 °C, the bulk conductivities increase to 1.6×10^{-5} and 1.33×10^{-5} S cm^{-1}, which are about two orders of magnitude higher than that at room temperature. The Arrhenius plots of **EuL** and **DyL** for the bulk phase are linearly approximated, and the activation energy (E_a) was estimated to be 0.91 eV and 0.87 eV, respectively (Fig. 2b and Fig. S10, ESI†). The values possibly imply that the conduction takes place through the Vehicle Mechanism (0.5–0.9 eV),[12] and the proton movement takes place with the aid of a moving "vehicle".[13] The free water molecules accept protons which are dissociated from free carboxylic groups and/or coordination water molecules, forming H_3O^+. Then H_3O^+ move along one definite direction, while unladen vehicles (H_2O) move along the opposite direction to complete the proton transport (Fig. S11, ESI†).

The luminescent properties of the powered samples were investigated at room temperature. As shown in Fig. S13a (ESI†), the emission spectra of the Eu–Tb codoped MOF $\mathbf{Eu_xTb_{1-x}L}$ with different doping concentrations show characteristic transitions of both Eu(III) and Tb(III) ions. Upon doping Eu(III) to the **TbL** complex, the CIE coordinates of the complexes were tuned from the green to yellow, orange, and red region by varying the original molar ratio of Eu(III)/Tb(III) in the starting materials (Fig. S13b, ESI†). Additionally, the emissions of **LnL** (Ln = Eu, Tb, Dy) can be enhanced by the dilution of Gd(III) (Fig. S14, ESI†). By precise control of the proportion of Dy–Eu and Dy–Sm in the Gd analog, tunable white light emission could be successfully achieved. The emission spectra of $\mathbf{Dy_xEu_yGd_{1-x-y}L}$ and $\mathbf{Sm_xDy_yGd_{1-x-y}L}$ under excitation at 293 nm are shown in Fig. 3a and b. All the CIE coordinates almost fall in the white region (Fig. 3c and d). The CIE coordinates of the codoped compounds are summarized in Tables S3 and S4 (ESI†). Besides, the emission lifetime and quantum yield of **LnL**s and doped materials showed that **TbL** has the longest lifetime of 653 μs and highest quantum yield of 42.2%, and the results are summarized in Table S5 (ESI†).

In conclusion, the successful synthesis and functional investigation of the material demonstrate that LnMOFs may behave as a kind of promising multi-functional material. It is expected that the opportunity of developing sensors and other devices using such functional LnMOFs could be realized, in which each function could be dynamically linked or controlled by the external stimulus.

The authors are grateful for the financial aid from the National Natural Science Foundation of China (Grant No. 91122030 and 21210001), '863'-National High Technology

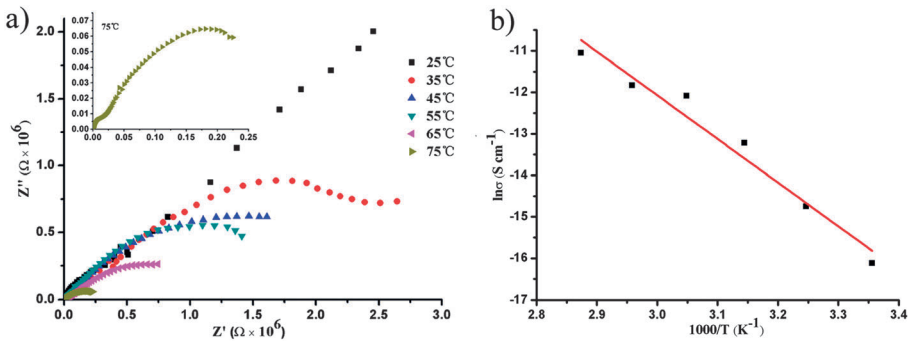

Fig. 2 (a) Nyquist plots of **EuL** from 25 °C C to 75 °C (inset: 75 °C); (b) temperature dependency of the bulk proton conductivity of **EuL**.

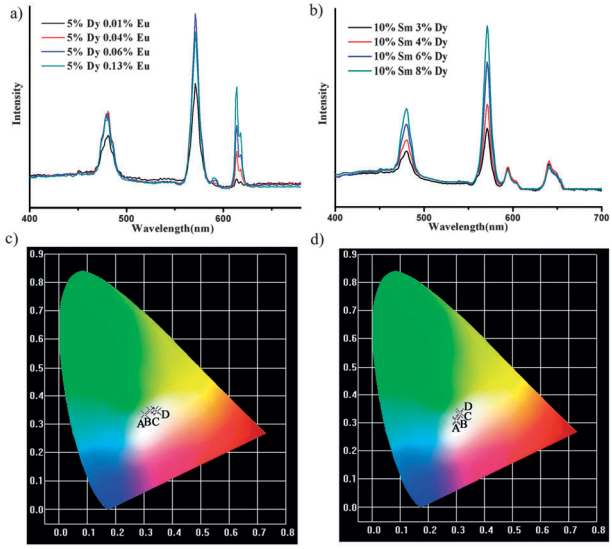

Fig. 3 (a) PL emission spectra of the Dy–Eu doped Gd compounds; (b) PL emission spectra of the Sm–Dy doped Gd compounds (λ_{ex} = 293 nm); (c) CIE chromaticity diagram for the $\mathbf{Dy_xEu_yGd_{1-x-y}L}$: (A) x = 0.05, y = 0.0001; (B) x = 0.05, y = 0.0004; (C) x = 0.05, y = 0.0006; (D) x = 0.05, y = 0.0013; (d) CIE chromaticity diagram for the $\mathbf{Sm_xDy_yGd_{1-x-y}L}$: (A) x = 0.1, y = 0.03; (B) x = 0.1, y = 0.04; (C) x = 0.1, y = 0.06; (D) x = 0.1, y = 0.08.

Research and Development Program of China (Grant No. 2011AA03A407) and National Natural Science Foundation for Creative Research Group (Grant No. 21221061).

Notes and references

1 (*a*) J. Tian, L. V. Saraf, B. Schwenzer, S. M. Taylor, E. K. Brechin, J. Liu, S. J. Dalgarno and P. K. Thallapally, *J. Am. Chem. Soc.*, 2012, **134**, 9581; (*b*) Z. J. Zhang, L. P. Zhang, L. Wojtas, P. Nugent, M. Eddaoudi and M. J. Zaworotko, *J. Am. Chem. Soc.*, 2012, **134**, 924; (*c*) G. C. Xu, W. Zhang, X. M. Ma, Y. H. Chen, L. Zhang, H. L. Cai, Z. M. Wang, R. G. Xiong and S. Gao, *J. Am. Chem. Soc.*, 2012, **133**, 14948; (*d*) B. Nepal and S. Das, *Angew. Chem., Int. Ed.*, 2013, **52**, 7224; (*e*) P. Serra-Crespo, M. A. van der Veen, E. Gobechiya, K. Houthoofd, Y. Filinchuk, C. E. A. Kirschhock, J. A. Martens, B. F. Sels, D. E. De Vos, F. Kapteijn and J. Gascon, *J. Am. Chem. Soc.*, 2012, **134**, 8314.

2 (*a*) S. Bureekaew, S. Horike, M. Higuchi, M. Mizuno, T. Kawamura, D. Tanaka, N. Yanai and S. Kitagawa, *Nat. Mater.*, 2009, **8**, 831; (*b*) J. A. Hurd, R. Vaidhyanathan, V. Thangadurai, C. I. Ratcliffe, I. L. Moudrakovski and G. K. Shimizu, *Nat. Chem.*, 2009, **1**, 705; (*c*) H. Okawa, M. Sadakiyo, T. Yamada, M. Maesato, M. Ohba and H. Kitagawa, *J. Am. Chem. Soc.*, 2013, **135**, 2256; (*d*) V. G. Ponomareva, K. A. Kovalenko, A. P. Chupakhin, D. N. Dybtsev, E. S. Shutova and V. P. Fedin, *J. Am. Chem. Soc.*, 2012, **134**, 15640; (*e*) S. Sen, N. N. Nair, T. Yamada, H. Kitagawa and P. K. Bharadwaj, *J. Am. Chem. Soc.*, 2012, **134**, 19432.

3 M. Yoon, K. Suh, S. Natarajan and K. Kim, *Angew. Chem., Int. Ed.*, 2013, **52**, 2688.

4 (*a*) D. Umeyama, S. Horike, M. Inukai, Y. Hijikata and S. Kitagawa, *Angew. Chem., Int. Ed.*, 2011, **50**, 11706; (*b*) X. Q. Liang, F. Zhang, W. Feng, X. Q. Zou, C. J. Zhao, H. Na, C. Liu, F. X. Sun and G. S. Zhu, *Chem. Sci.*, 2013, **4**, 983; (*c*) M. Sadakiyo, H. Okawa, A. Shigematsu, M. Ohba, T. Yamada and H. Kitagawa, *J. Am. Chem. Soc.*, 2012, **134**, 5472.

5 (*a*) P. Falcaro and S. Furukawa, *Angew. Chem., Int. Ed.*, 2012, **51**, 8431; (*b*) N. B. Shustova, A. F. Cozzolino, S. Reineke, M. Baldo and M. Dinca, *J. Am. Chem. Soc.*, 2013, **135**, 13326; (*c*) D. F. Sava, L. E. S. Rohwer, M. A. Rodriguez and T. M. Nenoff, *J. Am. Chem. Soc.*, 2012, **134**, 3983; (*d*) X. T. Rao, T. Song, J. K. Gao, Y. J. Cui, Y. Yang, C. D. Wu, B. L. Chen and G. D. Qian, *J. Am. Chem. Soc.*, 2013, **135**, 15559.

6 (*a*) Y. J. Cui, Y. F. Yue, G. D. Qian and B. L. Chen, *Chem. Rev.*, 2012, **112**, 1126; (*b*) J. Rocha, L. D. Carlos, F. A. A. Paz and D. Ananias, *Chem. Soc. Rev.*, 2011, **40**, 926; (*c*) B. Chen, S. Xiang and G. Qiang, *Acc. Chem. Res.*, 2010, **43**, 1115; (*d*) M. D. Allendorf, C. Bauer, R. K. Bhakta and R. J. T. Houk, *Chem. Soc. Rev.*, 2009, **38**, 1330.

7 (*a*) F. Le Natur, G. Calvez, C. Daiguebonne, O. Guillou, K. Bernot, J. Ledoux, L. Le Pollès and C. Roiland, *Inorg. Chem.*, 2013, **52**, 6720; (*b*) P. R. Matthes, C. J. Höller, M. Mai, J. Heck, S. J. Sedlmaier, S. Schmiechen, C. Feldmann, W. Schnickc and K. Müller-Buschbaum, *J. Mater. Chem.*, 2012, **22**, 10179; (*c*) S. Dang, J. H. Zhang and Z. M. Sun, *J. Mater. Chem.*, 2012, **22**, 8868.

8 (*a*) J. M. Taylor, K. W. Dawson and G. K. H. Shimizu, *J. Am. Chem. Soc.*, 2013, **135**, 1193; (*b*) R. M. P. Colodrero, K. E. Papathanasiou, N. Stavgianoudaki, P. Olivera-Pastor, E. R. Losilla, M. A. G. Aranda, L. León-Reina, J. Sanz, I. Sobrados, D. Choquesillo-Lazarte, J. M. García-Ruiz, P. Atienzar, F. Rey, K. D. Demadis and A. Cabeza, *Chem. Mater.*, 2012, **24**, 3780.

9 (*a*) Reticular Chemistry Structure Resource (RCSR), http://rcsr.anu.edu.au./; (*b*) V. A. Blatov and A. P. Shevchenko, *TOPOS 4.0*, Samara State University, Russia; (*c*) Euclidean Patterns in Non-Euclidean Tilings (EPINET), http://epinet.anu.edu.au/.

10 (*a*) I. M. Hodge, M. D. Ingram and A. R. West, *J. Electroanal. Chem. Interfacial Electrochem.*, 1975, **58**, 429; (*b*) I. M. Hodge, M. D. Ingram and A. R. West, *J. Electroanal. Chem. Interfacial Electrochem.*, 1976, **74**, 125.

11 E. Barsoukov and J. R. Macdonald, *Impedance Spectroscopy*, Wiley Interscience, New York, 2005.

12 A. Shigematsu, T. Yamada and H. Kitagawa, *J. Am. Chem. Soc.*, 2011, **133**, 2034.

13 K. D. Kreuer, A. Rabenau and W. Weppner, *Angew. Chem., Int. Ed.*, 1982, **21**, 208.

